FLEXURAL CAPACITY OF COMPOSITE GIRDERS: DESIGN EQUATION ACCOUNTING FOR BRIDGE HIGH PERFORMANCE STEELS

Dang Viet DUC[1)] and Yoshiaki OKUI [1)]
[1] Structural Mechanics and Dynamics Lab., Department of Civil and Environmental Engineering, Saitama University

ABSTRACT

The bending moment capacity of a composite girder largely depends on local bucking of compressive components, such as flange plates and web plates. The current Japanese design equation for load-carrying capacity of compressive steel plates is examined for four conventional steel grades and new steel grades SBHS500 and SBHS700. Statistical distribution of the normalized compressive strength is obtained by means of Monte Carlo simulation in combination with the response surface which is obtained from sufficient number of FE simulation plate analyses. Both initial deflection and residual stress are considered as sources of variability. The mean values of normalized compressive strength in this study are similar to those obtained from experimental tests (Fukumoto and Itoh, 1984). The standard deviation of the current study exhibits about half of the experimental results (Fukumoto and Itoh, 1984) within the practical range $0.6<R<1.2$. The positive bending moment capacity of composite steel girders is examined through parametric study employing elasto-plastic finite element analyses. The web slenderness limits of section classification for homogeneous and hybrid girders with bridge high performance steel are explored. Beside, the effects of initial bending moment due to unshored construction method on the web slenderness limit are investigated. It is shown that the noncompact web slenderness limits in conventional design standards are conservative for composite sections. Many sections, which are classified as slender by current specifications, demonstrate sufficient flexural capacity as noncompact.

KEYWORDS: bridge high performance steels, compressive strength, local buckling, hybrid girder, web slenderness limit

1. INTRODUCTION

The steel-concrete composite girder is one of the most common supper-structural types for highway and railway bridges. In composite girders under un-shored construction method, which is very common for composite girders, first, a steel girder only resists a bending moment due to dead loads of steel and wet concrete. The local buckling of the top flange plate in the steel girder due to the initial bending moment critically dominates the flexural resistance of the composite girders in the construction state. Besides, application of bridge high performance steels SBHS500, SBHS700 and hybrid steel girders is expected to be an economical solution for composite girder bridges. Steels SBHS500 and SBHS700, with yield strengths of 500 and 700 MPa, respectively, have been standardized in 2008 in Japannese Industrial Standards (2008). They present the advantage of high yield strength, good weldability. However, if compared to conventional (normal) steels they possess different inelastic behavior, such as almost no yield plateau, smaller ductility, and a greater yield-to-tensile strength ratio. The bending moment capacity of a composite girder largely depends on local bucking of compressive components, such as flange plates and web plates. Hence, the compressive strength of simply supported steel plates and section classifications based on the web slenderness limits of composite girders with SBHS steels for homogeneous as well as hybrid sections are investigated in the current study.

The current compressive strength design equation for unstiffened plates in Japanese Specifications for Highway Bridge (JSHB) version 2002 (JSHB, 2002) has been originally proposed in 1980 (JSHB, 1980). This equation was based on experimental data for normal steel with yield strengths mainly less than 450 MPa. Hence, it is necessary to examine the applicability of the current compressive strength design equation of JSHB to steel plates with new steel grades.

Regarding the compressive strength design equation of JSHB, Usami and Fukumoto (1989),

Usami (1993), and Kitada et al. (2002) show that the design equation is un-conservative within the range 0.5<R<0.75 (intermediate range) and over-conservative in the range R>0.8 (slender range), in which R is the slenderness parameter. However, studies Usami and Fukumoto (1989) and Usami (1993) consider only the normal (SM490Y) steel plates and they employed the perfectly elstoplastic assumption for modeling the inelastic behavior of steel material.

For theses reasons, the compressive strength design equation of JSHB need to be examined and developed for SBHS steel grades. However all the referred studies were based on the deterministic method. The recent design specifications trend towards the partial safety factor method (ISO, 1998), in which a safety factor separates into individual causes, such as the variability on material property and the confidence of strength prediction method. The partial safety factor method with probability-based partial factors has been employed in Eurocode (CEN, 2004 and CEN, 1994), and AASHTO (AASHTO, 2007) as well. In order to determine the safety factors and the nominal compressive strength, statistical information, such as the mean value and standard distribution of the compressive strength, is necessary. Komatsu and Nara (1983) carried out a number of FE analyses of steel plates with considering initial deflection based on collected measurement data from actual steel bridges to obtain the mean value and standard deviation of compressive strength. However, this study considered only residual stress σ_{rc}/σ_y=0.3 as a deterministic quantity, where σ_{rc} is the compressive residual stress. (Fukumoto and Itoh (1984) proposed the mean (M) and mean minus twice standard deviation (M-2S) curves of the compressive strength on the basis of a database on single plate and box column compression test data. The M and M-2S curves also show that the current JSHB design equation for steel plates under compression is un-conservative within intermediate range and over-conservative in slender range. Fukumoto and Itoh (1984) also reported the statistical distribution of residual stress and initial deflection. However, this study also considered the steel plates with initial deflection $W_0/b > 1/150$, where W_0 and b are the maximum initial deflection and plate width, respectively.This study intends to examine the current JSHB design equation of steel plate compressive strength for normal and SBHS steels, and to evaluate the mean and standard deviation of compressive strength.

Application of SBHS500 to hybrid girders is expected to be an economical solution for composite girder bridges. AASHTO (AASHTO, 2005) employs the hybrid factor R_h to calculate the yield moment M_{yf} of a hybrid section from the yield moment M_y of the relevant homogeneous section. This hybrid factor was proposed based on studies by Subcommittee on Hybrid Beams and Girders (1968) and Schilling (1968). However, the using factor in the current AASHTO was derived from stress-strain distribution assumption of steel section only and not considered the effect of a initial bending moment. The initial bending moment is induced by wet concrete load in the case the bridge girders are constructed by un-shored method, which is a very common construction method. Therefore, a new hybrid factor formula will be developed in the present study.

The sequent part of the paper devotes to studying web slenderness limits for section classification of composite homogeneous and hybrid sections with SBHS500 under a positive bending moment. The bending moment capacity of a composite section largely depends on a section class and local bucking of components of steel sections. Since the possibility of local buckling is restricted only for the upper part of web plates for composite sections under a positive bending moment, the section classification is governed by a width thickness ratio of web plates under compression.

Table 1. Web slenderness limit given by Eurocode (CEN, 1996) and AASHTO (2005)

Section class	Flexural resistance	Web slenderness limit	
		AASHTO	Eurocode
Compact	$M_u \geq M_p$	$\frac{2D_{cp}}{t_w} \leqq 3.76\sqrt{\frac{E_s}{f_y}}$	$b_w/t_w \leq \begin{cases} \frac{41.5\varepsilon}{\alpha} & \alpha \leq 0.5 \\ \frac{456\varepsilon}{13\alpha - 1} & \alpha > 0.5 \end{cases}$
Noncompact	$M_p \geq M_u \geq M_y$	$\frac{2D_c}{t_w} < 5.7\sqrt{\frac{E_s}{f_y}}$	$b_w/t_w \leq \begin{cases} \frac{42\varepsilon}{0.67 + 0.33\psi} & \psi \geq -1.0 \\ 62\varepsilon(1-\psi)\sqrt{-\psi} & \psi \leq -1.0 \end{cases}$
Slender	$M_y \geq M_u$	Otherwise	Otherwise

E_s : elastic modulus of steel
f_y : Yield strength of steel

$\varepsilon = \sqrt{235/f_y}$

Other parameters are defined in Fig.1 a and b

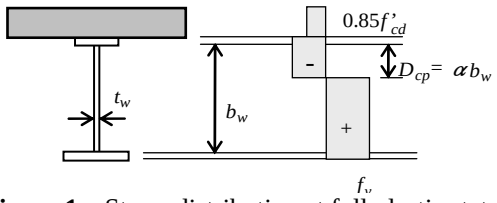

Figure 1a. Stress distribution at full plastic state in compact section

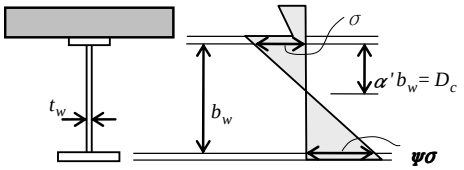

Figure 1b Stress distribution in noncompact and slender sections of homogeneous girders

Table 1 summarizes the section classification criteria in AASHTO Specifications and Eurocode, where M_u is the bending moment capacity of a composite section; M_p and M_y are the plastic moment and the yield moment, respectively. The symbols used in Table 1 are defined in Fig.1.

2. COMPRESSIVE STRENGTH OF STEEL PLATES

2.1. Examination of JSHB design equation

2.1.1 Plate properties

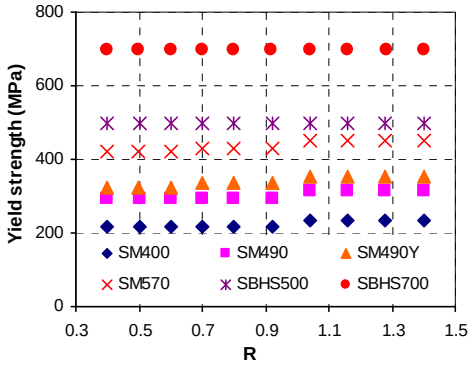

Figure 2. Slenderness parameter and yield strength in FE analyses

Four normal steel grades SM400, SM490, SM490Y, SM570 and two bridge high performance steel SBHS500, SBHS700 are considered in the current study. Fig. 2 shows yield strengths and slenderness parameters R considered in the FE analyses, where R is defined by

$$R = \frac{b}{t}\sqrt{\frac{\sigma_y}{E}\cdot\frac{12(1-\mu^2)}{\pi^2 k}} \qquad (1)$$

where b, t, σ_y, E, μ, and k=4.0 stand for the plate width, thickness, yield strength, elastic modulus, poison ratio, and buckling coefficient, respectively. The aspect ratio of all steel plates is assigned to 1.

2.1.2. FEM model

Nonlinear FE analysis considering both material and geometric nonlinearity is conducted. Prandtl-Reuss equation is employed to model the steel plasticity. The idealized uniaxial stress-strain relationships used in the numerical analyses are shown in Fig.3.

Regarding the boundary condition, all four edges of a plate model are assigned as simple supports. Figure 4 shows the distributions of residual stress and initial deflection assumed in the FE analysis. The probabilistic distributions of residual stress and initial deflection are based on measurement data reported by Fukumoto and Itoh (1984).

The displacement control method is used to apply the compressive stress. ABAQUS S4R shell elements are used for plate FE model with mesh size of 30x30 elements.

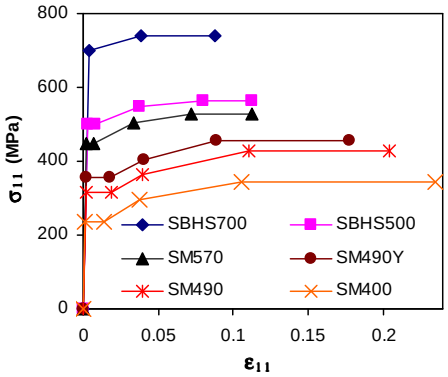

Figure 3. Idealized stress-strain relations of steel grades considered in current study

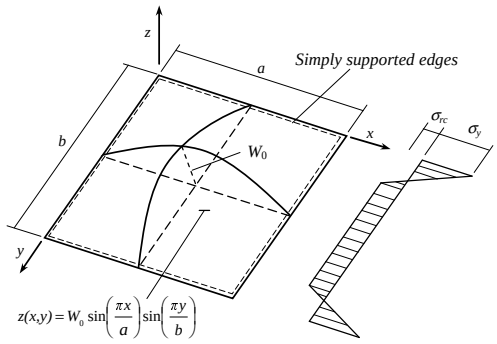

Figure 4. Idealized residual stress distribution and sinusoidal initial deflection surface

2.1.3. Comparison of FE results with experimental results

The normalized compressive strengths obtained from the FE analyses as well as past experimental results (Dwight and Moxham, 1969 and Rasmussen and Hancock, 1992) are plotted in Fig. 4 as a function of R. In these analyses, an initial deflection W_0/b = 1/150 and a residual stress σ_{rc}/σ_y = 0.4 are considered as a conservative

assumption. As shown in figure 5, the FEM results lay the lower bound of experimental results, which corresponds to the conservative assumption.

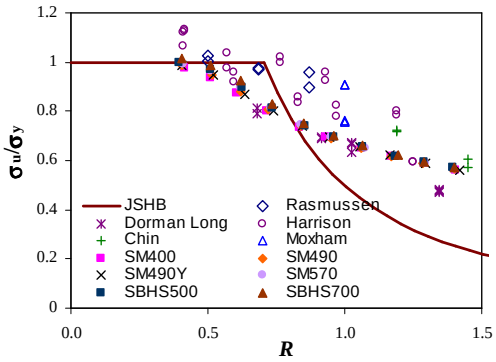

Figure 5. Comparison of current study results to previous test results

2.1.4. Compressive strength of different steel grades

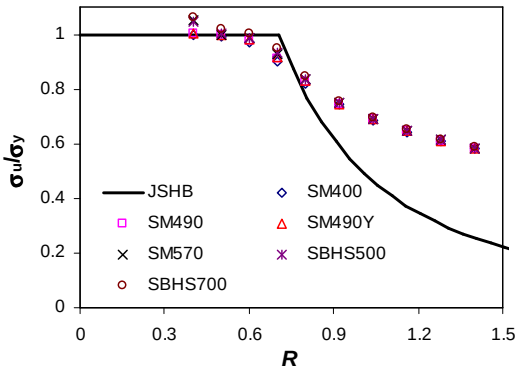

Figure 6. Normalized compressive strength of plate with 6 steel grades in the case W_0/b=1/400 and σ_{rc}/σ_y=0.23

In this section, the normalized compressive strengths of different steel grades are compared in the case of mean values of the residual stress and the initial deflection. The mean values of normalized residual stress and initial deflection are obtained as σ_{rc}/σ_y=0.23 and W_0/b=1/400, respectively from the measurement data reported in Fukumoto and Itoh (1984). In the evaluation of the mean value of the normalized initial deflection, the measurement data for W_0/b>150 are excluded owing to an allowable fabrication upper limit in JSHB.

As shown in figure 6, the compressive strengths of steel plates with 6 steel grades are quite similar in the whole range of R. The largest difference occurs at R ≈ 0.7 and R ≈ 0.4, and the normalized compressive strength of SBHS700 steel plates (maximum value among 6 steel grades) is about 6% greater than that of the SM400 steel plates (minimum value among 6 steel grades). For R > 0.4, the compressive strength of SBHS steel plates with larger YR value is greater than that of normal steel plate with lower YR value.

2.2. Compressive strength scatterness

2.2.1. Response surface

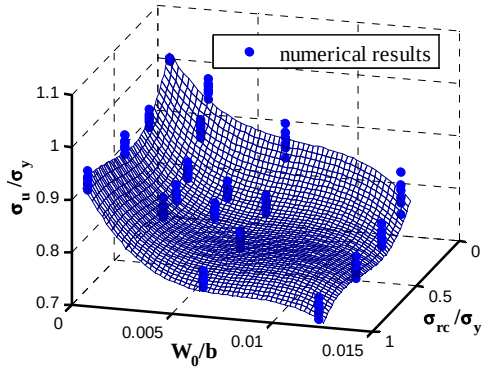

Figure 7. The response surface shape presented along with FEM results for the case R = 0.8

To obtain the probability distribution of the compressive strength, Monte Carlo method is employed. However, to obtain a convergent result in the Monte Carlo simulation, it is essential to implement a large number of deterministic analyses, and accordingly it would take long time. Hence, to overcome this problem, a response surface of the normalized compressive strength, which is an approximate algebraic function of the initial deflection and residual stress, is instead of the deterministic analyses. The current study employs ten response surfaces corresponding to the 10 considered R values.

Table 2: Constant values of 10 Response surfaces

R value	p_{00}	p_{01}	p_{02}	p_{03}	p_{10}	p_{11}	p_{12}	p_{20}	p_{21}	p_{30}
0.40	1.098	-40.22	5442.0	-248100	0.007	-2.320	-48.4	-0.007	2.25	0.000
0.50	1.034	-15.15	1683.0	-90660	-0.012	-8.400	-42.4	0.069	6.72	-0.057
0.60	1.012	-1.72	-1894.0	100500	-0.087	-21.150	507.9	0.284	11.01	-0.198
0.70	1.037	-34.54	3169.0	-135000	-0.234	-32.100	1465.0	0.568	9.74	-0.342
0.80	1.047	-65.98	8382.0	-389100	-0.584	-0.520	1309.0	1.006	-15.13	-0.492
0.92	0.963	-40.44	3081.0	-112100	-0.937	57.210	-891.1	1.368	-35.91	-0.632
1.04	0.850	-23.31	1188.0	-34700	-0.788	47.270	-769.2	1.169	-29.12	-0.556
1.16	0.757	-12.66	377.6	-11430	-0.567	25.720	46.8	0.856	-20.27	-0.419
1.28	0.697	-10.08	367.4	-12430	-0.435	23.330	-269.2	0.617	-15.11	-0.288
1.40	0.650	-7.44	229.3	-8387	-0.343	18.580	-208.5	0.462	-11.63	-0.211

The response surface is expressed as a simple algebraic function,

$$\overline{\sigma}_u = p_{00} + p_{10}\overline{\sigma}_r + p_{01}\overline{W}_0 + p_{20}\overline{\sigma}_r^{\,2} + p_{11}\overline{\sigma}_r\overline{W}_0 + \\ + p_{02}\overline{W}_0^{\,2} + p_{21}\overline{\sigma}_r^{\,2}\overline{W}_0 + p_{12}\overline{\sigma}_r\overline{W}_0^{\,2} + p_{30}\overline{\sigma}_r^{\,3} + p_{03}\overline{W}_0^{\,3} \quad (2)$$

where $\overline{\sigma}_u = \sigma_u / \sigma_y$, $\overline{W}_0 = W_0 / b$ and $\overline{\sigma}_r = \sigma_{rc} / \sigma_y$.

The constants p_{ij} in equation 2 were determined from a set of 114 deterministic FE results for each steel grade and R value by using the least square method.

Figure 7 shows an obtained response surface along with FE numerical results for R=0.8. All constants of ten response surfaces are presented in Table 2. The obtained response surfaces show good fit for numerical results in the cases R≥0.7 with the coefficient of determination (R-square) > 95%. For R<0.7, the R-square values become slightly lower due to the influence of the hardening of high strength steels (SM570, SBHS500, SBHS700).

2.2.2. Stochastic inputs of initial imperfections

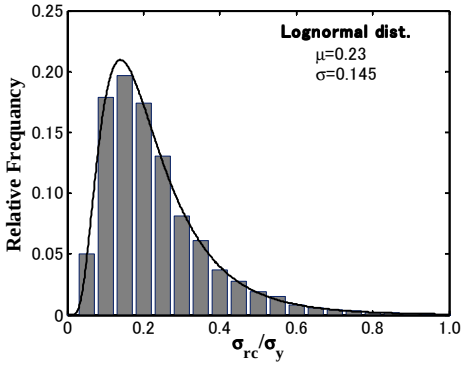

Figure 8. Generated random input of initial deflection

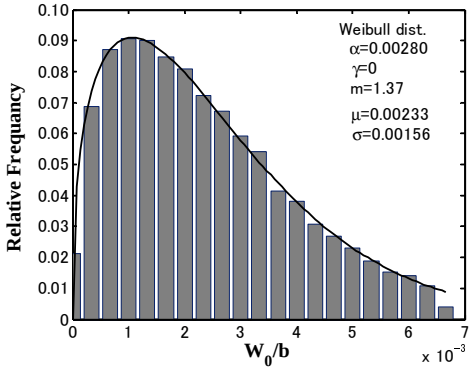

Figure 9. Generated random input of residual stress

In the Monte Carlo simulation, the probabilistic distribution of the initial deflection is assumed as the Weibull distribution, and the residual stress as the Lognormal distribution as shown in figure 8 and 9 (Fukumoto and Itoh,1984). In this figure, the generated random variables in the Monte Carlo simulation are also plotted as the histogram chart. The generated normalized initial defections more than W_0/b>1/150 are excluded in the simulation due to an allowable fabrication upper limit in JSHB.

The probabilistic distribution of compressive strengths is obtained by application of the response surface and a large number of random inputs of residual stress and initial deflection. The converged mean and standard deviation are obtained by processing 10000 random input couples of residual stress and initial deflection. The histogram of compressive strength with 10000 random input couples in the case of R=0.8 is shown in figure 9. Results of 10 convergent mean and standard deviation of compressive strengths are presented in Table 2.

2.2.3. Results of Monte Carlo simulation

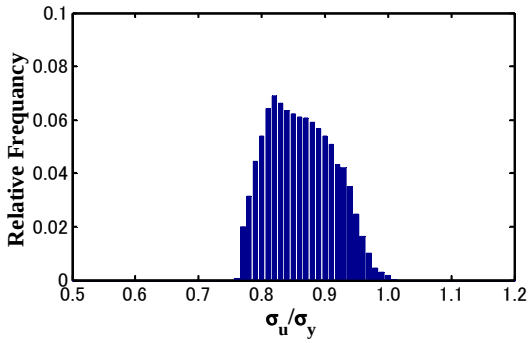

Figure 10. Probability distribution of compressive strength for R=0.8

The probabilistic distribution of compressive strengths is obtained by application of the response surface and a large number of random inputs of residual stress and initial deflection. The converged mean and standard deviation are obtained by processing 10000 random input couples of residual stress and initial deflection. The histogram of compressive strength with 10000 random input couples in the case of R=0.8 is shown in figure 10. Results of 10 convergent mean and standard deviation of compressive strengths are presented in Table 3.

Table 2: Mean and standard deviation of normalized compressive strength

R value	0.4	0.5	0.6	0.7	0.8	0.92	1.04	1.16	1.28	1.4
M value	1.039	1.006	0.982	0.938	0.862	0.766	0.701	0.653	0.617	0.586
S value	0.0277	0.0157	0.0212	0.0413	0.0515	0.0399	0.0294	0.0216	0.0171	0.0145

In figure 11, the mean values of normalized compressive strength with error bar equal to two times the standard deviation are plotted along with the current JSHB design equation, mean (M) curve and mean minus 2 standard deviation (M-2S) curve proposed in Fukumoto and Itoh (1984).

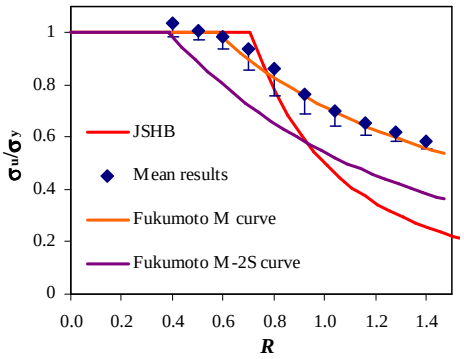

Figure 11. Comparison between current study, JSHB, 2002, and Fukumoto and Itoh (1984) results

As shown in figure 11, the mean values of normalized compressive strength are similar to the mean curve reported in Fukumoto and Itoh (1984), which was proposed from test results. Within $0.65 \leq R \leq 0.85$, the mean values of the current study are slightly greater than that reported in Fukumoto and Itoh (1984). One of the possible reasons is that the current study does not consider steel plates with $W_0/b > 1/150$ and the influence of initial deflection on compressive strength is more significant within the mentioned range of R than other ranges. Also seen in Fig.9, the M-2S curve proposed in Fukumoto and Itoh (1984) is too conservative if compared to corresponding results of the current study.

A comparison of standard deviation of compressive strengths obtained in the current study and previous study Fukumoto and Itoh (1984) is presented in Fig.12. Within the practical range $0.6 < R < 1.2$, the standard deviations of the current study exhibit about half of reported values in Fukumoto and Itoh (1984). As seen in the figure, the standard deviations obtained by the current study have a clearer tendency, and attained to the maximum value at $R \approx 0.8$. Within the range $0.7 < R < 0.9$, the ultimate state of compressive plates is elasto-plastic buckling, and accordingly the compressive strength is significantly influenced by both residual stress and initial deflection. For $R > 0.9$, the standard deviation decreases, and the elastic buckling becomes dominant. The residual stress has almost no effect on the compressive strength. For $R < 0.7$, the compressive strength tends to attain the yield strength and is mainly influenced by initial deflection. In particular for $R < 0.5$, the hardening behavior of high strength steel (SM570, SBHS500 and SBHS700) starts to have a significant effect on the compressive strength.

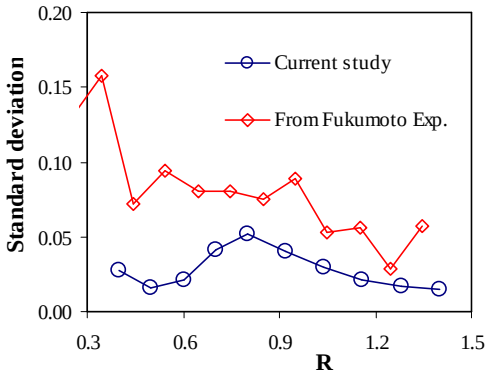

Figure 12. Comparison of standard deviation values obtained in current study and reported in Fukumoto and Itoh (1984)

3. SECTIONS CLASSIFICATION FOR COMPOSITE GIRDERS

3.1. Nonlinear FE model

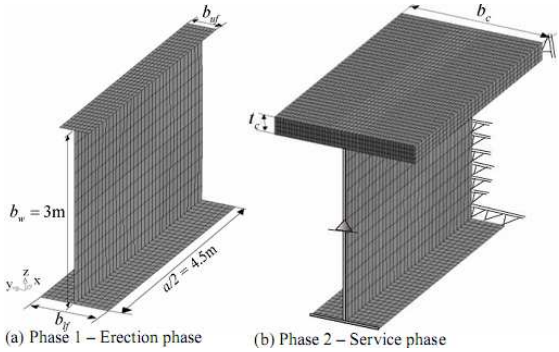

Figure 13. FE models for phase analysis

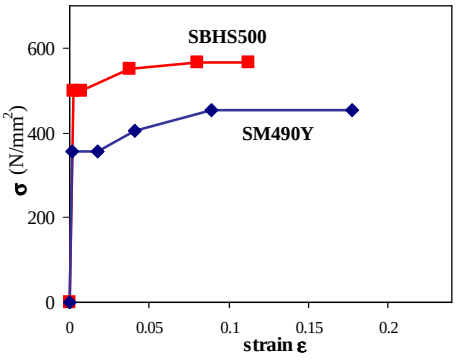

Figure 14. Uniaxial stress-strain relation applied for steel material models

A half of the steel-concrete composite I-girders are meshed based on symmetry of the model structure and loading condition. The flanges and web are modeled by 4-node thin shell elements; concrete slab is modeled with 8-node solid elements. To simulate the unshored construction method, the phase analysis is employed as shown in Fig.13. The effect of initial bending moment can be considered in the phase analysis. The magnitudes of the initial bending

moment are assigned to M_1 = 0.2; 0.4; 0.6 M_{ys}, where M_{ys} is the yield bending of steel girder section only.

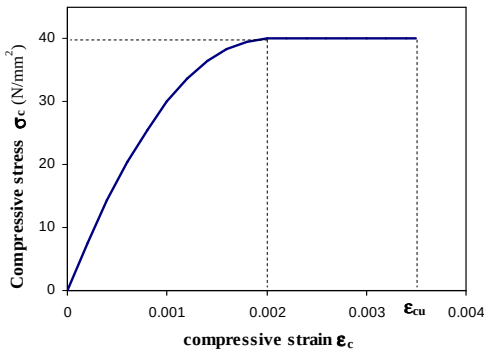

Figure 15. Compression uniaxial stress-strain curves applied for concrete material model

The displacement control method is used in the incremental nonlinear analysis. The longitudinal displacements of the girder end is prescribed to apply a uniform bending moment incrementally. The elasto-plastic steel material behavior is modeled similarly with the model presented in subsection 2.1.2. The uniaxial multi-linear stress-strain curves of steel grade SM490Y for the web plate and SBHS500 for the flange plates are shown in Fig.14, which are based on experimental results. Concrete in compression is modeled as linear-elastic, plastic hardening material and Mohr-Coulomb yield criterion. The uniaxial stress-strain curve for concrete under compression is shown in Fig.15 (JSCE, 2007).

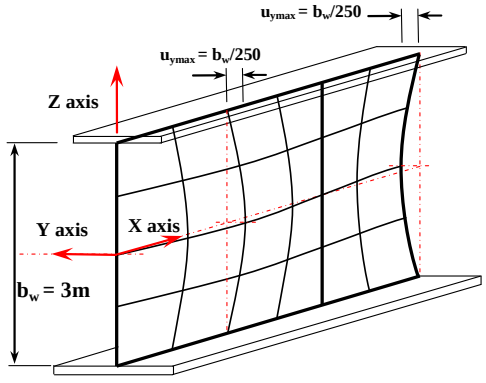

Figure 16. Geometric imperfection in web plate

The initial geometric imperfection in the web plate is considered as a sinusoidal form as defined in Eq.(3). The maximum initial out-of-plane displacement is assigned to b_w/250 according to Japanese "Specifications for Highway Bridges" (Japan Road Association, 2002):

$$u_y = \frac{b_w}{250}\sin\left(\frac{\pi}{b_w}z\right)\cos\left(\frac{\pi}{b_w}x\right) \tag{3}$$

where u_y, b_w, x, y, z are explained in Fig.16.

3.2. Proposal of hybrid factor

In the current study, a hybrid factor for composite girders will be proposed with accounting for the effect of initial bending moment due to un-shored construction method. In this construction method, first the initial bending moment M_1 due to the dead load at construction stages is applied to steel sections alone and then bending moment M_2 due to the live load is done to composite sections, as shown in Fig.17. The hybrid factor is developed for positive bending moment only, and for sections where bottom web yields first.

The yield moment of a composite hybrid section M_{yf} is estimated by subtracting the reduced contribution due to the prior yielding at web plate M' from the yield moment of the relevant composite homogeneous section M_y:

$$M_{yf} = M_y - M' = M_1 + M_2 - M' \tag{4}$$

where $M_y = M_1 + M_2$ is the yield moment of the homogeneous steel section.

The hybrid factor is defined as the ratio of M_{yf} to M_y, and expressed as

$$R_h = \frac{M_{yf}}{M_y} = \frac{M_1 + M_2 - M'}{M_y} \tag{5}$$

$$R_h = \Phi S_{1.tf}\left(\frac{1}{S_{2.bf}} - \frac{1}{S_{1.bf}}\right) + 1 - (2+\alpha)(1-\alpha)^2 \left\{\frac{h}{1+\left[\Phi + \left(1 - \frac{\Phi y_s}{h - y_s}\right)\left(\frac{h}{y_c} - 1\right)\right]}\right\}^2 \frac{t_w}{3S_{2.bf}} \tag{6}$$

$$\alpha = \frac{f_{yw}}{f_{yf}}$$

where $S_{1.tf}$, $S_{1.bf}$, and S_{2bf} are section modulus of steel section with respect to the top and bottom flanges, and that of composite section with respect to the bottom flange, respectively. f_{yw} and f_{yf} are the yield strength of web plate and flange plate, respectively. Φ represents the ratio of M_1 to the yield moment M_{ys} of homogeneous steel section only.

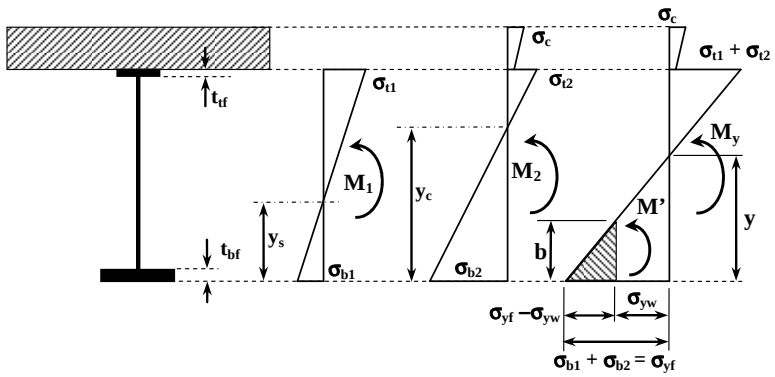

Figure 17. Assumption on stress distributions for estimation of hybrid yield moment; (a) Initial bending moment on steel section alone, (b) Bending moment on composite section, (c) Superposed stress distribution

3.3. Results and discussion

3.3.1. SBHS500 homogeneous section

The following figures will present the FE analysis results of SBHS500 homogeneous girders along with the web slenderness limit of AASHTO, Eurocode and the previous results (Gupta et al., 2006), in which b_w/t_w and α present the width-thickness ratio and the parameter of the compression region of web plate, respectively.

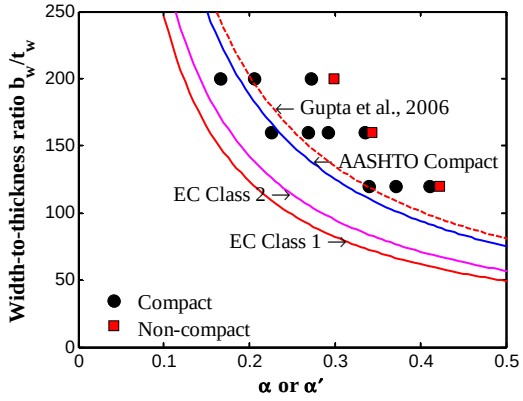

Figure 18. Compact-noncompact limit of homogeneous SBHS500 steel section (M_1=0)

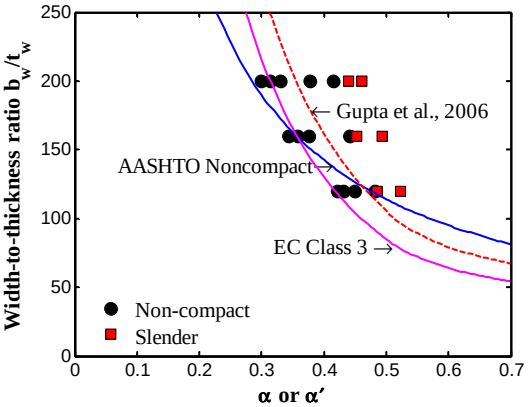

Figure 19. Noncompact-slender limit of homogeneous SBHS500 steel sections (M_1=0)

In Fig.18, the black symbols stand for the numerical results judged as compact sections, while the red ones for noncompact sections. The SBHS500 homogeneous sections for the initial bending moment M_1=0 present significant greater web slenderness limit than those of AASHTO, Eurocode and proposed by Gupta et al. The inelastic behavior of SBHS500 steel seems to be the main reason. Owing to the smaller yield plateau of SBHS500, it can sustain a greater plastic local bucking strength than conventional steel.

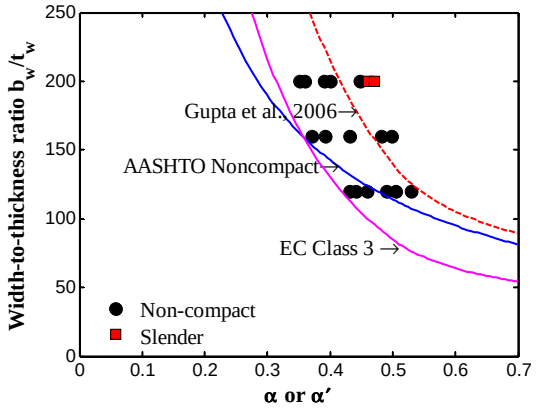

Figure 20. Noncompact-slender limit of homogeneous SBHS500 steel sections (M_1=0.4M_{ys})

Gupta et al. (2006) reported the considerable effect of M_1 on the noncompact-slender limit. Fig. 20 and 21 show the numerical results for the web slenderness limit of noncompact-slender boundary for initial bending moments of M_1 = 0.4, 0.6 M_{ys}, respectively. In these figures, the black symbols denote FE results classified as noncompact sections, while the red ones do slender sections. With increasing the initial bending moment, the web slenderness limit of noncompact-slender boundary increases, which presents the same trend as reported by Gupta et al. (2006).

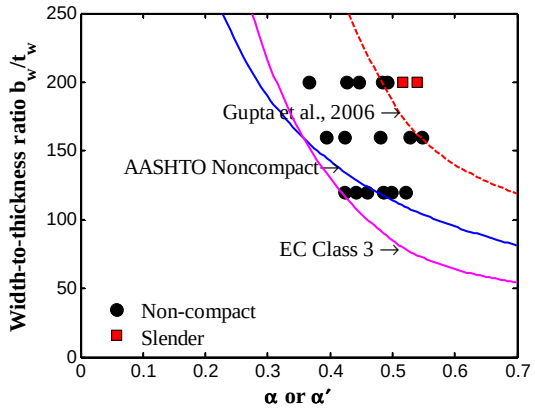

Figure 21. Noncompact-slender limit of homogeneous SBHS500 steel sections (M_1=0.6M_{ys})

3.3.2. SBHS500-SM490Y hybrid sections

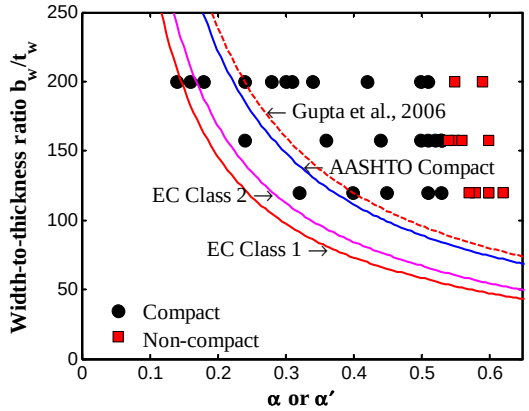

Figure 22. Compact-noncompact limit of hybrid SBHS500-SM490Y steel sections (M_1=0)

Fig.22 shows comparison between FE results for SBHS500-SM490Y hybrid sections and the compact-noncompact slenderness limits of AASHTO and Eurocode. The FE results present the larger compact-noncompact slenderness limit than those of AASHTO and Eurocode. In addition, comparing between Fig.18 and 22, the web slenderness limit for hybrid sections is even greater than that for homogeneous SBHS500 steel sections.

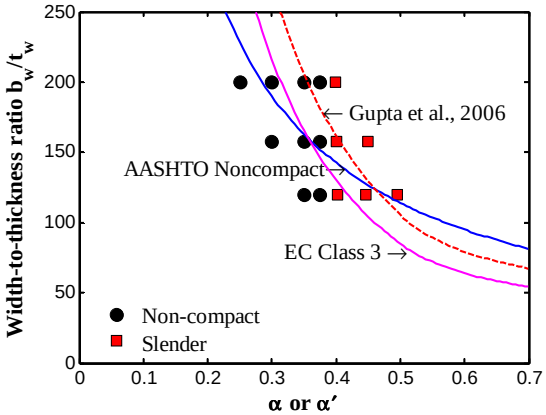

Figure 23. Noncompact-slender limit of composite SBHS500-SM490Y hybrid steel section (M_1=0)

Fig.23 shows the noncompact-slender limit without the initial bending moment. In this section, the yield moment M_y of a hybrid section is defined as the result of yield bending moment of a corresponding homogeneous section multiplied by the hybrid factor. Comparing the homogeneous sections shown in Fig. 19, it is shown that the web slenderness limit for hybrid sections is lower than that of homogeneous sections. The noncompact-slender limit boundary of this case is almost vertical.

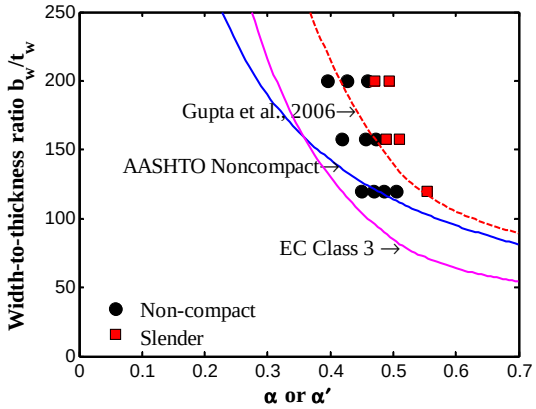

Figure 24. Noncompact-slender limit of hybrid SBHS500-SM490Y steel section (M_1=0.4M_{ys})

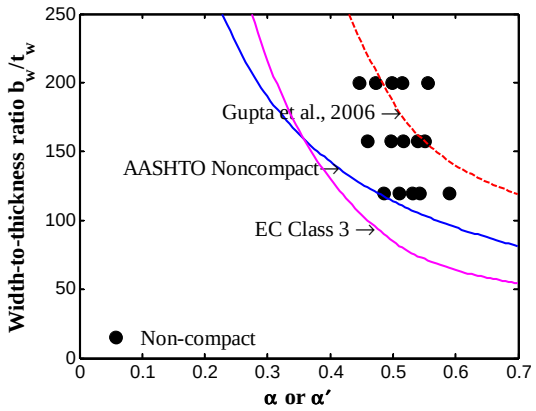

Figure 25. Noncompact-slender limit of hybrid SBHS500-SM490Y steel section (M_1=0.6M_{ys})

Fig. 24 and 25 illustrate FE results under initial bending moments of 0.4M_{ys} and 0.6M_{ys}, respectively. For M_1 = 0.4M_{ys}, the web slenderness limit for hybrid sections is lower than that of homogeneous sections as well. The difference is about 10%. Hence, considering initial bending moment with $M_1 \leq 0.4M_{ys}$ the web slenderness limit for the hybrid sections is about 10% lower than that of homogeneous sections. As shown in Fig. 25 there is no FE result judged as slender sections. It means that the composite girders with hybrid SBHS500-SM490Y steel sections always be classified as noncompact sections in practical range

of α or α' with considering high level of initial bending moment M_1.

4. CONCLUSIONS AND REMARKS

4.1. Compressive strength of steel plates

The mean values of normalized compressive strength of the steel plate obtained in the current study are similar to those proposed by Fukumoto and Itoh (1984), but slightly greater within the range $0.7<R<0.9$. The standard deviation of compressive strength obtained in this study is about half of values obtained from the experimental data reported in (Fukumoto and Itoh, 1984) within a range of $0.6<R<1.2$. The M-2S curve proposed in (Fukumoto and Itoh, 1984) is too conservative if compared to corresponding values obtained in the current study. The results of M-2S of the current study show that the current load-carrying-capacity JSHB design equation of steel plates is un-conservative within the range $0.5 < R < 0.8$ and over-conservative for $R > 0.85$.

Within the range of slenderness parameter $0.4 \leq R \leq 1.4$, the normalized compressive strengths of normal steel and SBHS steel are similar for the same levels of R and initial imperfections. However, compressive strength of steel plates with SBHS grades with greater YR is slightly greater than that of normal steel grades.

4.2. Web slenderness limit for composite section classification

Applying SBHS500 steel to both homogeneous and hybrid sections can extend significantly the web slenderness limits for section classification.

The noncompact-slender web slenderness limit for hybrid sections is about 10% lower than that of homogeneous sections.

For high level of initial bending moment M_1, the composite girders with hybrid SBHS500-SM490Y steel sections always be classified as noncompact sections in practical range of α or α'.

With the application of SBHS500 steel to both composite homogeneous and hybrid girders, the web plate of steel girder can be designed with higher width-to-thickness ratio than requirements of current specifications as AASHTO and Eurocode.

REFERENCES

American Association of State Highway and Transportation Officials (2005) "*AASHTO LRFD bridge design specification,*"

American Association of State Highway and Transportation Officials (2007) "*AASHTO LRFD bridge design specification – Fourth edition,*"

CEN, Eurocode3 (2004) "*Design of Steel Structures, Part 1-5, plated structural elements*" European Committee for Standardization, Brussels, Belgium

CEN, Eurocode4 (1994) "*Design of Composite Steel and Concrete Structures, Part 2, General rules and rules for bridges*," European Committee for Standardization, Brussels, Belgium

Dwight, J, B., Moxham, K, E. "Welded steel plates in compression." *The Structural Engineer*, Vol. 47, No. 2, pp. 49-66, 1969

Fukumoto, Y. and Itoh, Y. (1984). "Basic compressive strength of steel plates from test data." *Proc. of JSCE*, No. 334/I-1, pp. 129-139

Gupta, V.K., Okui, Y., and Nagai, M. (2006) "Development of web Slenderness Limits for Composite I-Girders accounting for Initial Bending Moment", *Doboku Gakkai Ronbunshuu A*, Vol.62, No.4, 854-864.

ISO 2394 (1998). "*General principles on reliability for structures*," 3rd Ed., International Standard.

Japan Road Association (1980) "*Specifications for Highway Bridges – part II. Steel Bridges*,"

Japan Road Association (2002) "*Specifications for Highway Bridges – part II. Steel Bridges*,"

Japanese Industrial Standard (2008) "*JIS G 3140, Higher yield strength steel plates for bridges*"

Japan Society of Civil Engineers - JSCE (2007) "*Standard Specifications for Concrete Structures* -2007*"*

Kitada, T., Yamaguchi, T., Matsumura, M., Okada, J., Ono, K., and Ochi, N. (2002) "New technology of steel bridge in Japan." *Journal of Constructional Steel Research*, 58, pp. 21-70.

Komatsu, S. and Nara, S. (1983) "Statistical study on steel plate members." *Journal of Structural Engineering, ASCE*, 109(4), pp. 977-992.

Rasmussen, K. J. R. and Hancock, J. G. (1992). "Plate slenderness limits for high strength

steel sections." *J. Construct. Steel Research*. 23, pp. 73-96.

Schilling, G. (1968) "Bending Behavior of Composite Hybrid Beams," *Journal of the Structural Division, ASCE*, 94, ST8, pp. 1945-11964, 1968

Subcommittee on Hybrid Beams and Girders (1968) "Design of Hybrid Steel Beams." *Journal of the Structural Division, ASCE*, 94, ST6, pp. 1397-1426.

Usami, T. and Fukumoto, Y. (1989). "Deformation analysis of locally buckled steel compression members." *Journal of Constructional Steel Research*, 13, pp. 111-135.

Usami, T. (1993) "Effective width of locally buckled plates in compression and bending." *Journal of Structural Engineering, ASCE*, Vol. 119, No. 5, pp. 1358-1373.